

Magnetic Properties of Amorphous Particles Produced by Spark Erosion

A. E. Berkowitz, J. L. Walter, and K. F. Wall

General Electric Corporate Research and Development Center, Schenectady, New York 12301

(Received 23 January 1981)

The magnetizations and Curie temperatures of amorphous particles produced by spark erosion are found to be greatly reduced from the values for amorphous ribbons of the same compositions. The differences increase as particle size decreases. This behavior is interpreted as a decrease of chemical short-range order in the particles as a result of their faster quenching rate. Anomalous low-field behavior in the critical region also supports this conclusion.

PACS numbers: 75.50.Kj, 75.30.Cr, 76.80.+y

In recent investigations of amorphous magnetic alloys of transition metals with metalloids, the samples have generally been ribbons prepared by chill casting from the melt.¹ Ribbons of the same compositions produced in different laboratories or samples of the same compositions produced by other methods have shown no significant differences.² Hence the properties of the ribbons have seemed to embody the characteristics of the amorphous state for transition-metal-metalloid alloys. We have prepared amorphous particles by the spark-erosion method^{3,4} in the Fe-B, Fe-Si-B, and Fe-Co-Si-B systems and have found that their magnetic properties differ significantly from those of amorphous ribbons of the same compositions produced by the chill-casting technique.¹ This Letter reports on the properties of the Fe₇₅Si₁₅B₁₀ system, which appears to be typical of the alloys investigated.

The spark-erosion method for producing amorphous particles consists essentially of maintaining a spark discharge between two electrodes immersed in a dielectric fluid.⁴ The electrodes were fabricated from the alloys of interest and the dielectric fluid was dodecane [CH₃(CH₂)₁₀CH₃]. The Fe₇₅Si₁₅B₁₀ starting alloy was prepared by melting and casting, under argon, 99.91% Fe, 99.8% B, and Si with 1-ppb impurities. As a result of the spark discharge, small regions of the electrodes were rapidly heated above the melting temperature, whereupon molten droplets or vaporized portions were ejected into the dielectric fluid and were then rapidly quenched into the amorphous state. The particles were generally spherical and those with diameters >0.5 μm were readily washed free of organic material. Size fractions in the range from 0.5 to 30.0 μm were prepared by sieving. Amorphous ribbon was prepared by the chill-casting method from the same starting alloy. The ribbon was ~30 μm thick and ~0.85 mm wide.

There were no significant differences among the x-ray diffraction patterns from the amorphous particles or ribbon. The centroids and line widths of the two broad maxima were virtually the same for all these samples. Insufficient sample ruled out chemical analysis so composition was determined from properties measured after crystallization in vacuum and N₂ at 800 °C for 24 h. The equilibrium crystalline phases of the Fe₇₅Si₁₅B₁₀ alloy are Fe₂B and Fe_{78.6}Si_{21.4},⁵ and only these phases were detected by x-ray diffraction on crystallized samples. *T_c* values (determined from low-field temperature sweeps) were the same as those for Fe₂B and Fe_{78.6}Si_{21.4} and the saturation magnetizations for crystalline samples of all particle sizes and ribbon were consistent with the value for the equilibrium alloy. Composition was most accurately determined from analyses of the Mössbauer spectra of crystallized samples. The spectra were analyzed in terms of four sextets: one measured on an Fe₂B sample and three⁶ used to fit the spectrum from an Fe_{78.6}Si_{21.4} sample. This showed that none of the crystallized particle or ribbon samples deviated by more than 0.8 at.% from the nominal alloy composition. As a further check, an alloy of composition Fe₇₅Si₁₆B₉ was analyzed by the same method which yielded Fe_{75.3}Si_{16.2}B_{8.5}. Thus the x-ray, magnetization, and Mössbauer data showed that there were no significant composition differences among the various size fractions of the amorphous particles and the amorphous ribbon.

Isothermal magnetization measurements near *T_c* produced slight changes in the magnetic properties of the samples. This behavior is generally attributed to structural relaxation.⁷ The samples were therefore stabilized before the magnetization measurements with a preanneal at 733 K for 30 min. After this treatment, there were no significant changes in magnetic properties as a result of the isothermal measurements. This pre-

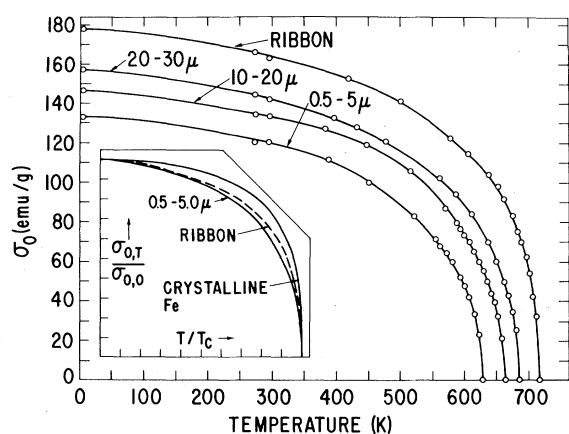


FIG. 1. $\sigma_0(T)$ derived from isothermal magnetization curves as described in the text. The inset shows reduced magnetization.

anneal increased $T_c < 15$ K from values measured on as-prepared samples. The mean hyperfine field, H_{mean} , increased $\sim 2\%$. These changes are much smaller than the differences among the samples tested.

Magnetization was measured in fields up to 80 kOe for $T \leq 273$ K; for $T > 273$ K, the maximum field was 25 kOe. At sufficiently low temperatures the isothermal magnetization curves were linear at high fields, and the spontaneous magnetization, $\sigma_0(T)$, could be obtained by extrapolating back to $H=0$. Near T_c , $\sigma_0(T)$ was determined by extrapolating plots⁸ of $\sigma^{2.5}$ vs $(H/\sigma)^{0.75}$.

In Fig. 1, $\sigma_0(T)$ is shown for the amorphous ribbons and for three size fractions of the amorphous particles. The most remarkable feature of these data are the marked decreases in T_c and $\sigma_0(4.2$ K) for the particles as compared to the

ribbon. T_c and $\sigma_0(4.2$ K) for the largest particles, whose diameters are similar to the ribbon thickness, are significantly lower than the corresponding value for the ribbon, and these quantities continue to decrease with decreasing particle diameter. The values are listed in Table I. The value of $2.01 \mu_B$ for the moment per Fe atom (μ_{Fe}) for the ribbon is typical for this concentration of metalloids, but the moment is reduced by 24% in the smallest particles, with an accompanying decrease of 89 K in T_c . Reduced thermomagnetic data are shown in the inset in Fig. 1. The stronger temperature dependence of the reduced magnetization of the amorphous samples compared to crystalline Fe has often been noted.

Mössbauer spectra were measured at 295 and 77 K fitted with a distribution of hyperfine fields, $p(H)$, determined by the Fourier-series method of Window.⁹ The results are shown in Fig. 2. The spectra clearly indicate a reduction in average hyperfine field and an increase in linewidth from the ribbon through the smaller particles. The plots of $p(H)$ demonstrate these trends and show that the increased half width at half maximum (HWHM) is primarily due to the increasing probability of low hyperfine field as the particle size decreases. Some data derived from the $p(H)$ are listed in Table I. The last two columns in Table I demonstrate the very close proportionality between σ and H_{mean} .

In the crystalline Fe-B system,¹⁰ it has been shown that both μ_{Fe} and H_{mean} are principally determined by the number of nearest-neighbor metalloids. A similar metalloid dependence was observed for H_{mean} in crystalline Fe-Si.¹¹ Furthermore, in the amorphous Fe-B system,¹⁰ it was possible to reproduce the dependence of μ_{Fe} and

TABLE I. Magnetic and Mössbauer data from amorphous $\text{Fe}_{75}\text{Si}_{15}\text{B}_{10}$ particles and ribbon.

Sample	4.2K			T_c (K)	295K				
	σ_0 (emu/gm)	μ_{Fe}^a (μ_B)	μ_{Fe}^a $\mu_{\text{Fe, ribbon}}$		$H_{\text{mean}}^{a,b}$ (kOe)	$H_{\text{peak}}^{a,c}$ (kOe)	HWHM ^a (kOe)	$\frac{H_{\text{mean}}^d}{H_{\text{mean, ribbon}}}$	$\frac{H_{\text{mean}}(295\text{K})^d}{H_{\text{mean}}(77\text{K})}$
Ribbon	178.8	2.01	1.0	717	235	240	86	1.0 (1.0)	.90 (.93)
20-30 μm	157.9	1.78	.89	685	208	213	102	.89 (.87)	.93 (.91)
10-20 μm	147.7	1.66	.83	664	193	203	107	.82 (.82)	.92 (.92)
0.5-5.0 μm	134.8	1.52	.76	628	175	192	114	.74 (.84)	.90 (.91)

^a Estimated uncertainty is $\pm 2\%$ for σ_0 and μ_{Fe} , ± 5 kOe for H_{mean} , ± 3 kOe for H_{peak} , and ± 2 kOe for HWHM.

^b $H_{\text{mean}} = \int H p(H) dH$.

^c H_{peak} is the hyperfine field corresponding to the maximum in $p(H)$.

^d Value in parentheses is corresponding ratio of μ_{Fe} .

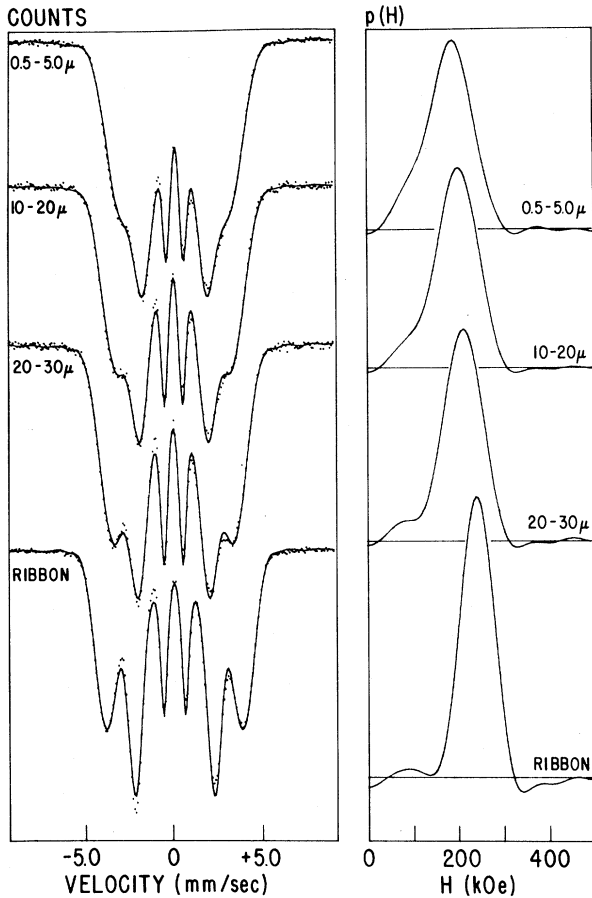


FIG. 2. Fitted Mössbauer spectra taken at 295 K. Hyperfine field distributions, $p(H)$.

H_{mean} on B concentration with use of the nearest-neighbor-dependent values from the crystalline alloys in a model with strong chemical short-range order (CSRO). Likewise in the amorphous Fe-Si system, the nearest-neighbor Si concentration seemed to determine μ_{Fe} ¹² and H_{mean} .¹³ In all these cases μ_{Fe} and H_{mean} decreased with increasing nearest-neighbor metalloid concentration. Thus one may conclude that the changes in μ_{Fe} and $p(H)$ from the ribbon through the particles are the result of a corresponding increase in metalloid concentration around Fe sites. This implies a reduction of CSRO for the particles compared to the ribbon and a further reduction as the particles decrease in size. We suggest that the reduced CSRO is the result of a faster quenching for the particles ($>10^7$ K/sec)¹⁴ compared to the ribbon (10^6 K/sec)¹ and an increasing quenching rate for decreasing particle diameter.¹⁵ Furthermore, <10 - μm amorphous spherical particles of the same composition produced by gas atomiza-

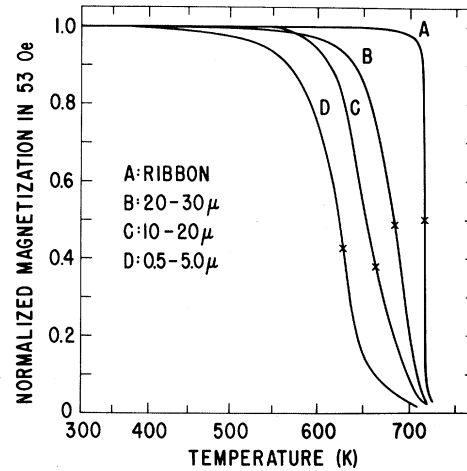


FIG. 3. Magnetization as a function of temperature measured in 53 Oe and normalized to the value at 295 K. Crosses indicate T_c 's determined from the high-field data in Fig. 1.

tion with water quenching (quench rate 10^5 to 10^6 K/sec)¹⁶ were virtually identical to the thicker ribbon in all properties. Thus the magnetic properties are determined by quenching rate; particle size is a factor only as it relates to the quenching rate.

Figure 3 shows the temperature dependence of the magnetization in 53 Oe normalized to the 295-K value. Normalized curves for all fields ≤ 100 Oe were the same as those in Fig. 3. The crosses on each curve indicate T_c determined from the high-field data in Fig. 1. The very broad transitions in the critical region for the particles are surprising in view of the conventional behavior of the extrapolated high-field data in Fig. 1 near T_c . The broad transitions do not result from a size-dependent distribution of T_c values among particles in a given size fraction; the same breadth was present for size distributions only 1- μm wide. The curves for the particles all have tails which extrapolate to the T_c for the ribbon. This suggests that the increasing HWHM and shift of H_{mean} with decreasing particle size results from increasing heterogeneity in the local magnetic environment within a particle. Thus the greater CSRO in the ribbon would be consistent with local regions of similar chemical configuration magnetically ordering at the same temperature. With decreasing CSRO in the particles, there would be an increased temperature range over which critical fluctuations are important. However, it is not clear why the low-field data are so much more sensitive to the magnetic het-

erogeneity than are the extrapolated high-field data.

Thus the amorphous particles produced by spark erosion appear to have a significantly higher degree of chemical disorder than do amorphous ribbons of the same composition because of the higher quench rate from the liquid. The decreased CSRO is reflected in lower μ_{Fe} , T_c , H_{mean} , and other consistent changes in $p(H)$. An anomalously wide transition in the critical region in low applied fields is puzzling in view of a more regular behavior in the critical region in high fields. However, it is clear from the above that amorphous ribbon represents only one class of the amorphous state.

We are grateful for the assistance of A. L. Ortiz, Jr., W. E. Rollins, R. P. Goehner, D. W. Marsh, and C. H. Reilly. We appreciate useful discussions with C. L. Chien, W. P. Wolf, A. Aharoni, L. M. Levinson, and L. J. Schowalter.

¹J. L. Walter, in *Rapidly Quenched Metals, III*, edited by B. Cantor (The Metals Society, London, 1978), Vol. 1, pp. 30-33.

²A. S. Schaafsma, I. Vincze, F. Van der Woude, T. Kemeny, and A. Lovas, *J. Phys. (Paris), Colloq.* **41**, C8-246 (1980).

³T. Yamaguchi and K. Narita, *IEEE Trans. Magn.* **13**, 1621 (1977).

⁴A. E. Berkowitz and J. L. Walter, in *Rapid Solidification Processing, II*, edited by R. Mehrabian, B. H. Kear, and M. Cohen (Claitor's Publication Division, Louisiana, 1980), pp. 294-305.

⁵A. E. Berkowitz, J. D. Livingston, B. D. Nathan, and J. L. Walter, *J. Appl. Phys.* **50**, 1754 (1979).

⁶M. B. Stearns, *Phys. Rev.* **129**, 1136 (1963).

⁷H. N. Ok and A. H. Morrish, *Phys. Rev. B* **22**, 3471 (1980).

⁸A. Arrott and J. E. Noakes, *Phys. Rev. Lett.* **19**, 786 (1967).

⁹R. Window, *J. Phys. E* **4**, 401 (1971).

¹⁰I. Vincze, D. S. Boudreaux, and M. Tegze, *Phys. Rev. B* **19**, 4896 (1979).

¹¹C. Blaauw, H. Hansen, F. van der Woude, and G. A. Sawatsky, in *Proceedings of the Fifth International Conference on Mössbauer Spectroscopy*, edited by M. Hud and T. Zercik (Czechoslovakian Atomic Energy Commission, Prague, 1975), p. 10.

¹²G. Marchal, Ph. Mangin, M. Piecuch, Chr. Janot, and J. Hubsch, *J. Phys. F* **7**, L165 (1977).

¹³G. Marchal, Ph. Mangin, M. Piecuch, and Chr. Janot, *J. Phys. (Paris), Colloq.* **37**, C6-763 (1976).

¹⁴J. L. Walter and A. E. Berkowitz, unpublished.

¹⁵N. J. Grant, in *Rapid Solidification Processing*, edited by R. Mehrabian, B. H. Kear, and M. Cohen (Claitor's Publishing Division, Louisiana, 1978), p. 230.

¹⁶S. A. Miller and R. J. Murphy, *Scripta Metall.* **13**, 673 (1979).

Spin Waves in a Disordered Medium: A Simple Model with a Mobility Edge

J. Canisius and J. L. van Hemmen

Universität Heidelberg, D-6900 Heidelberg 1, Federal Republic of Germany

(Received 20 January 1981)

A computer simulation of an isotopically disordered harmonic crystal with positive and negative masses is presented. This system may be related to a Heisenberg-Mattis random magnet, for which our results give the elementary excitations. Ideas of percolation theory are employed to explain the existence of a mobility edge in two and three dimensions whenever the positive or negative masses, but not both, percolate. For the corresponding random magnet this implies a new kind of magnon spectrum in which localized and extended states coexist.

PACS numbers: 75.10.Jm, 63.50.+x

Spin waves are *delocalized* boson excitations. They were found¹ as elementary excitations in quantum spin Heisenberg models describing ordered media with translational invariance. However, it has remained unclear whether spin waves can exist in a disordered medium without translational invariance or a well-defined wave vector \vec{k} . To examine this question we consider the Heisenberg-Mattis model^{2,3} of a random magnet,

characterized by the Hamiltonian

$$\mathcal{H} = - \sum_{i,j} \xi_i \xi_j J_{ij} \vec{S}(i) \cdot \vec{S}(j). \quad (1)$$

The $J_{ij} = J(|i-j|) \geq 0$ represent a finite-range interaction on a d -dimensional cubic lattice, and the ξ_i 's are independent, identically distributed random variables taking values $+1$ and -1 with probabilities p and $q = 1 - p$, respectively. Fixing